A Designed Protein with Packing between Left-Handed and Right-Handed Helices†

Samuel K. Sia‡,§ and Peter S. Kim*,‡

Howard Hughes Medical Institute, Whitehead Institute for Biomedical Research, Department of Biology, Massachusetts Institute of Technology, Nine Cambridge Center, Cambridge, Massachusetts 02142, and Committee on Higher Degrees in Biophysics, Harvard University, Cambridge, Massachusetts 02138

Received April 10, 2001

ABSTRACT: A common motif in protein structures is the assembly of α-helices. Natural α-helical assemblies, such as helical bundles and coiled coils, consist of multiple right-handed α-helices. Here we design a protein complex containing both left-handed and right-handed helices, with peptides of D- and L-amino acids, respectively. The two peptides, D-Acid and L-Base, feature hydrophobic heptad repeats and are designed to pack against each other in a "knobs-into-holes" manner. In solution, the peptides form a stable, helical heterotetramer with tight packing in the most solvent-protected core. This motif may be useful for designing protease-resistant, helical D-peptide ligands against biological protein targets.

The interfaces between interacting right-handed α-helices are structurally well characterized. Among the most studied α-helical assemblies (*1*) is the coiled coil, which consists of two to five interacting α-helices that wrap around each other with an overall superhelical twist (*2*). A distinguishing structural feature of coiled coils is the specific and regular local packing of side chains ("knobs-into-holes"), a feature first predicted by Crick using helical net diagrams (*3*). Helical net diagrams depict the packing of side chains of interacting helices, where the side chain of one helix ("knob") fits into a cavity ("hole") formed by the side chains of the partnering helix. While their relevance for describing interhelical packing in globular proteins is debatable (*4*, *5*), helical net models are accurate structural representations of coiled coils, which contain a regular and extensive packing interface. The two key structural predictions of helical net diagrams, an interhelix packing angle (Ω) of 20° and knobs-into-holes packing of side chains (Figure 1A), have been confirmed by crystal structures of coiled coils (*6*, *7*).

Coiled coils are attractive targets for protein design because of their structural regularity and functional diversity. Early work on simple, designed coiled coils (*8*) led to numerous studies on controlling the oligomeric state (*7*, *9*, *10*), parallel versus antiparallel interhelical orientation (*11*, *12*), selective heteromeric partnering (*13*, *14*), native-like packing (*13*, *15*, *16*), ligand-induced conformational switches (*17*, *18*), and superhelical twist (*19*).

While much work focuses on designing helical assemblies and coiled coils that contain right-handed α-helices (*20*), little is known about engineering proteins that contain both left-handed and right-handed α-helices. Such a motif would add a new structural element to the current repertoire of designed proteins, and may be useful in designing protease-resistant helical D-peptide inhibitors (which can form left-handed helices) that bind helical L-protein targets. In this report, we set out to design a helical assembly containing both left-handed helices and right-handed helices (consisting of D- and L-amino acids, respectively).

Because this "D/L" assembly is necessarily heteromeric rather than homomeric, we use as the basis for our design a previously engineered heteromeric system called Acid/Base (*13*, *21*). The Acid and Base peptides were identical in sequence except for residues at the **e** and **g** positions [for a heptad repeat of the form (**abcdefg**)$_n$]; these residues are Glu in Acid and Lys in Base. Two sets of Acid/Base peptides were previously studied (*13*, *21*). The Acid-p1/Base-p1 peptides contain hydrophobic Leu residues at their interface (**a** and **d** positions), except for a single polar residue, Asn 14, in both peptides (*13*). Acid-p1/Base-p1 forms a parallel heterodimer with native-like packing in the hydrophobic core. In a subsequent study, Asn 14 was replaced with Leu 14 in both peptides (Acid-pLL/Base-pLL) (*21*). Acid-pLL/Base-pLL, which contains all Leu residues at the **a** and **d** positions, forms a very stable heterotetramer, but lacks a unique structure.

Here we design and study two peptides containing all Leu residues at the **a** and **d** positions: D-Acid and L-Base (consisting of D- and L-amino acids, respectively). We demonstrate that these peptides interact to form a stable helical tetramer. We also show that the heterotetramer exhibits both specific and nonspecific packing in its hydrophobic core.

MATERIALS AND METHODS

Peptide Synthesis and Purification. Peptides were synthesized by standard Fmoc chemistry with acetylated N-termini and amidated C-termini (sequences shown in Figure 1C). The identities of all peptides were confirmed by matrix-assisted laser desorption ionization mass spectroscopy (MAL-

† This research was supported by a grant from the National Institutes of Health (GM44162). S.K.S. was supported by the Howard Hughes Medical Institute Predoctoral Fellowship and the National Science and Engineering Council of Canada Postgraduate Fellowship.

* To whom correspondence should be addressed. Present address: Merck Research Laboratories, 770 Sumneytown Pike, West Point, PA 19486. Fax: (215) 993-1770. E-mail: peter_kim@merck.com.

‡ Massachusetts Institute of Technology.

§ Harvard University.

10.1021/bi010725v CCC: $20.00
Published on Web 06/30/2001

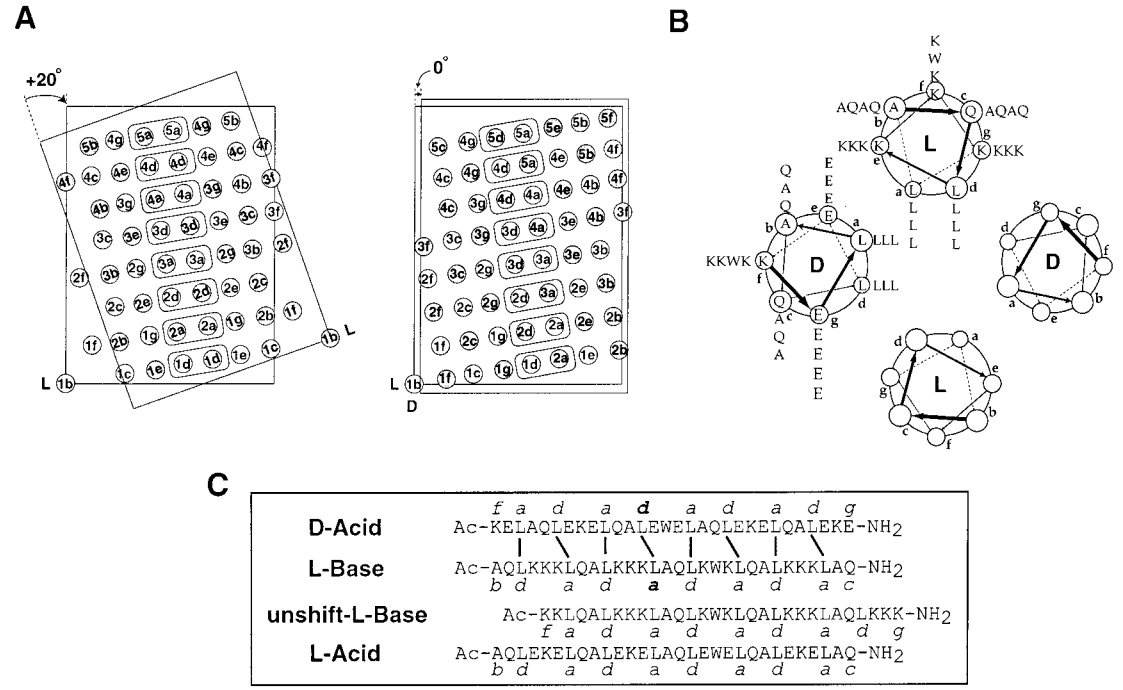

FIGURE 1: Design principles for packing a left-handed helix against a right-handed helix. (A) Helical net diagrams (*3*) showing the knobs-into-holes packing between two right-handed helices (L,L; left) and between left-handed and right-handed helices (L,D; right). The circles indicate the positions of Cα atoms, and the letters identify the heptad positions. In both cases, the right-handed helix is in the back (unshaded circles) and the helix in front is represented by shaded circles. While an interhelical packing angle of 20° is observed for packing two right-handed helices, 0° (or 180°) is the only solution for packing left-handed (D-amino acids) and right-handed (L-amino acids) helices while preserving knobs-into-holes packing and maintaining extensive interfacial contact. The hydrophobic interactions in each core layer are boxed. (B) Helical wheel projection (looking from the N-terminus) of a D/L tetramer, based on the Acid/Base system (*13*, *21*). While similar to helical wheel projections of natural coiled coils, the two helices rotate in opposite directions. The arrangement of the D- and L-helices shown here is predicted to minimize electrostatic repulsion. (C) The amino acid sequences of D-Acid, L-Base, shift-L-Base, and L-Acid are shown along with their heptad positions (italics). Predicted interactions between hydrophobic residues of D-Acid and L-Base are indicated by dark lines. The bold heptad positions indicate the Leu → Asn substitutions for the D-Acid-p1 and L-Base-p1 variants.

DI-MS)[1] (Perceptive Biosystems Voyager Elite) to be within 0.1% of the predicted masses. Reverse-phase high-performance liquid chromatography (HPLC) (Vydac C18 column) was used to purify the peptides. Peptide concentrations were determined by absorbance in 6 M guanidine hydrochloride, assuming extinction coefficients at 280 nm of 5690 M^{-1} cm^{-1} for Trp and 120 M^{-1} cm^{-1} for oxidized Cys (*22*).

Circular Dichroism (CD) Spectroscopy and Urea Denaturation. CD spectra were measured on an Aviv 62DS spectrapolarimeter at 25 °C in phosphate-buffered saline (PBS) [10 mM sodium phosphate and 150 mM NaCl (pH 7.0)] with a total peptide concentration of 10 μM.

For denaturation experiments, urea stock solutions were prepared daily and the concentration was determined by refractometry. To enhance the CD signal-to-noise ratio, 40 and 80 μM peptide solutions were used with an averaging time of 100 s per data point. The baselines were estimated by nonlinear fitting to the standard six-parameter two-state transition curve using weighted averages. With the fitted baselines, the fraction of unfolded peptide (f_u) at each urea concentration was determined and the equilibrium constant of folding (K_{fold}) was calculated according to the equation $K_{fold} = 4(1 - f_u)/(f_u^4 c^3)$, where c is the total peptide concentration (K_{fold} describes the heterotetrameric equilibrium $2D + 2L = D_2L_2$, where D is D-Acid and L is L-Base). The standard folding free energy ($\Delta G°_{fold}$) was obtained from the relationship $\Delta G° = -RT \ln K_{fold}$, where R is the gas constant and T is temperature. The linear extrapolation method then yields the $\Delta G°_{fold}$ at 0 M urea.

A competition experiment of D-Acid versus L-Acid for their mutual partner L-Base was performed with each peptide at 10 μM [L-Acid in this report is termed "Acid-pLL" (*21*)]. The CD spectrum of the mixture containing all three peptides was fit to the equation $\theta_{observed} = f_D(\theta_{DL} + \theta_L) + (1 - f_D)(\theta_{LL} + \theta_D)$, where f_D is the fraction of the L-Base bound to the D-Acid and θ is the CD ellipticity in millidegrees of different species (DL is D-Acid/L-Base, L is L-Acid, LL is L-Acid/L-Base, and D is D-Acid), assuming that all L-Base was bound to Acid peptides.

Sedimentation Equilibrium. Sedimentation equilibrium was performed using a Beckman XL-A analytical ultracentrifuge. Samples were dialyzed overnight against PBS. Rotor speeds of 30 000 and 40 000 rpm were used. Wavelengths corresponding to absorbance values between 0.1 and 1 were chosen. Partial molar volumes, solvent densities, and a correction to partial molar volume at 8 M urea were calculated as described previously (*23*). Global fitting of multiple rotor speeds was performed with the program MacNONLIN (*24*). Residuals for D-Acid/L-Base were either random or indicative of slight association.

[1] Abbreviations: MALDI-MS, matrix-assisted laser desorption ionization mass spectroscopy; HPLC, high-performance liquid chromatography; CD, circular dichroism; c_M, concentration of denaturant at which half the peptides are unfolded; LC−MS, liquid chromatography−mass spectroscopy; MW, molecular weight; ANS, 1-anilinonaphthalene-8-sulfonic acid; pD_{read}, pH measurement in D_2O uncorrected for isotope effect.

Nuclear Magnetic Resonance (NMR) Spectroscopy. One-dimensional ^{1}H NMR spectra were collected on a Bruker AMX 500 spectrometer at 25 °C. Samples were 500 μM (total peptide concentration) in PBS (pH 7.0) in a 90% H_2O/10% D_2O mixture. For amide-proton exchange experiments, a lyophilized 1:1 D-Acid/L-Base mixture was dissolved in D_2O and PBS (pD_{read} 6.4). Eighty scans were collected at each time point. To calculate the observed protection factor, the half-life of the most slowly exchanging amide protons (8.3 ppm) was estimated to be 3 h, giving an observed exchange rate (k_{ex}) of 6.4×10^{-5} s^{-1}. The intrinsic exchange rate (k_{int}) for a random coil at this temperature and pD is 12 s^{-1} (as calculated from ref *25* using the low-salt limit and corrected for pD_{read} and temperature; 12 s^{-1} is the rate for the most slowly exchanging amide protons after correction for the primary structure effect). The observed protection factor is calculated as k_{int}/k_{ex}.

The protection factor predicted from global unfolding is calculated as $1/f_u$. f_u was calculated from the equation $K_{fold} = [4(1 - f_u)]/f_u^4c^3 = \exp(-\Delta G^\circ_{fold}/RT)$, where $c = 500$ μM and $\Delta G^\circ_{fold} = -29.3$ kcal/mol (determined from urea denaturation).

The predicted average α-proton chemical shifts for 100% α-helix, 100% β-strand, and 100% random coil were calculated using ref *26*, using the amino acid sequence of D-Acid and L-Base.

Fluorescence Spectroscopy. Fluorescence measurements were taken on a Hitachi F-4500 instrument at 22 °C. The total peptide concentration was 50 μM, and the 1-anilinonaphthalene-8-sulfonic acid (ANS) concentration was 5 μM. Different peptide concentrations from 5 to 100 μM were tested with identical rank orders. The excitation wavelength was 372 nm.

Equilibrium Disulfide Exchange. Oxidized L-Base (5 μM) with an N-terminal Trp-Cys-Gly-Gly sequence (L-Base-N; the additional Trp facilitates its identification) and 5 μM oxidized L-Base with a C-terminal Gly-Gly-Cys sequence (L-Base-C) were mixed with 10 μM D-Acid in redox buffer [50 mM Tris (pH 8.8), 500 μM reduced glutathione, and 200 μM oxidized glutathione] in an anaerobic chamber. After 24 h, the reaction was quenched with glacial acetic acid (final concentration of 50% v/v). The oxidized species were identified by liquid chromatography−mass spectroscopy (LC−MS) (Finnegan-mat LCQ), with all molecular masses agreeing with the predicted molecular masses to within 1 Da. The equilibrium concentrations of various parallel and antiparallel species were determined by integrating the peaks on an analytical HPLC system (Vydac C18) and normalizing for the extinction coefficients of the parallel and antiparallel species at 280 nm.

RESULTS

Design Principles. On the basis of the success of the helical net diagram for modeling two interacting right-handed helices, we use the helical net diagram to model the interaction of a right-handed helix with a left-handed helix. When applied to the packing of a right-handed helix with a left-handed helix, the helical net diagram predicts a different but unique solution; namely, the two helices of a D/L structure will pack at a packing angle of 0° (Figure 1A).

The helical net model of the D/L structure reveals two notable differences compared with interactions between natural right-handed helices in coiled coils. First, in natural coiled coils, the two helices cross at an Ω of 20° to attain a knobs-into-holes packing arrangement and acquire a superhelical twist that allows interfacial contact to be maintained for arbitrary lengths in sequence (Figure 1A). However, in a D/L structure, the packing angle of 0° between the two straight α-helices allows the hydrophobic residues of the two helices to interact without the need for an overall superhelical twist. In this model, the hydrophobic residues [at the first (**a**) and fourth (**d**) positions] on the two helices maintain interaction for approximately four heptads before they diverge away from the interface (Figure 1A).

Second, the model predicts that in a D/L structure, interactions in the core layers occur between the **a** and **d′**, and **d** and **a′**, positions, as opposed to the usual situation, between the **a** and **a′**, and **d** and **d′**, positions of natural coiled coils (boxed residues in Figure 1A). The heptad register of the two interacting peptides should therefore be shifted by a half-heptad to reflect this different mode of packing (positions **a** and **d** are a half-heptad apart). Failure to match heptad registers for two interacting peptides is predicted to result in a structure containing knobs-into-holes interactions, but with staggered helical ends of half-heptads.

On the basis of these structural considerations, two 30-residue peptides, D-Acid and L-Base, were designed. The sequences of the peptides were based on the previously studied heteromeric Acid-pLL/Base-pLL system, in which the core positions **a** and **d** are Leu and positions **e** and **g** are Glu for Acid and Lys for Base, respectively (*21*) (Figure 1B,C). L-Acid and L-Base in this study are identical to Acid-pLL and Base-pLL, respectively, which were previously studied (*21*). The D-Acid peptide is based on L-Acid (*21*), but is synthesized with D-amino acids. Although D-Acid displays a helical wheel identical to that of L-Acid, its amino acid sequence is not simply a D-version of L-Acid. This is due to the different handedness of the helix of D-Acid, and a half-heptad register shift in accord with the packing model (i.e., D-Acid starts at position **f**, compared with L-Base and L-Acid, which start at position **b**).

To test the importance of the half-heptad shift, we also synthesized a Base peptide, "unshift-L-Base," with an unshifted heptad register compared with D-Acid (i.e., unshift-L-Base, like D-Acid, starts at position **f**) (Figure 1C). In addition, we tested the effect of a single polar substitution in the hydrophobic core of the D/L structure with two additional peptides: D-Acid-p1 (Leu 13 in D-Acid to Asn 13) and L-Base-p1 (Leu 14 in L-Base to Asn 14) (bold positions in the sequences are shown in Figure 1C).

CD of D-Acid/L-Base. CD spectroscopy of D-Acid and L-Base indicates that the individual peptides are partially helical in solution (Figure 2A). Because of the presence of both D- and L-amino acids, CD spectroscopy of a 1:1 D-Acid/L-Base mixture yielded an expectedly small signal (Figure 2A). The small ellipticity of the mixture is different from the simple sum of the ellipticities of the two individual peptides, suggesting that D-Acid and L-Base interact in solution.

Oligomeric State of D-Acid/L-Base. Sedimentation equilibrium of a 1:1 D-Acid/L-Base mixture shows an apparent molecular mass close to that expected for a heterotetramer, with random residuals indicating a good fit to an ideal species model (Figure 2B). An apparent molecular mass close to

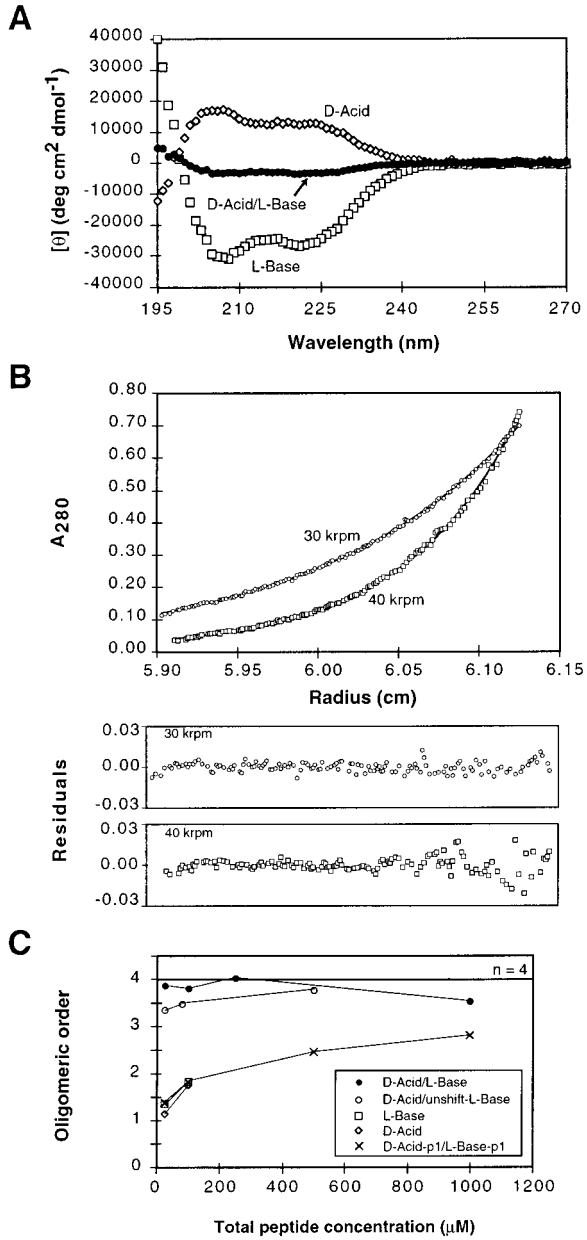

FIGURE 2: D-Acid and L-Base associate to form a heterotetramer. (A) CD spectra of D-Acid, L-Base, and a 1:1 mixture of D-Acid and L-Base in PBS at pH 7.0 and 25 °C. A peptide concentration of 10 μM was used in all cases. (B) Sedimentation equilibrium of D-Acid/L-Base. Shown is a 100 μM sample centrifuged at two different speeds (30 000 and 40 000 rpm). The global fit assuming a single ideal species is shown as a dark line (—). Residuals of the fit are shown in the bottom panel for the two rotor speeds. (C) Oligomeric state (apparent molecular weight relative to the average monomeric molecular weight) of various D-Acid and L-Base species as measured by sedimentation equilibrium analysis, as a function of total peptide concentration. The tetrameric state ($n = 4$) is highlighted.

that of the heterotetramer was obtained across a range of peptide concentrations (total peptide concentrations from 25 μM to 1 mM) (Figure 2C). The oligomeric state of D-Acid/L-Base is therefore the same as L-Acid/L-Base, which is also a stable heterotetramer (*21*).

Sedimentation equilibrium analysis shows that the individual D-Acid and L-Base peptides self-associate in a concentration-dependent fashion (Figure 2C). Moreover, fitting the sedimentation profiles of the individual peptides to idealized species results in nonrandom residuals, indicating an oligomeric equilibrium for the individual peptides, D-Acid and L-Base.

Effect of a Single Polar Interaction on the Oligomeric State of D-Acid-p1/L-Base-p1. In coiled coils, a single polar interaction in an otherwise fully hydrophobic core is often important for the formation of a specific structure. For example, a single buried asparagine interaction is important for forming a specific GCN4-p1 dimer (*6*, *7*) and a specific Acid-p1/Base-p1 dimer (*13*, *21*). As such, a single polar interaction was introduced into the D/L structure by the Leu 13 to Asn 13 mutation in D-Acid (D-Acid-p1) and the Leu 14 to Asn 14 mutation in L-Base (L-Base-p1) (bold positions in the sequences in Figure 1C). The introduction of a buried polar interaction expectedly destabilized the D/L structure as judged by a concentration dependence of the oligomeric state even at millimolar peptide concentrations (Figure 2C), and nonrandom residuals when fit to an idealized species model. However, D-Acid-p1/L-Base-p1 did not form a specific heterodimer as in the L version of Acid-p1/Base-p1 (*13*), and was not studied further.

Urea Denaturation of D-Acid/L-Base. The thermodynamic stability of the D-Acid/L-Base heterotetramer was determined by urea denaturation and fit to a monomer−tetramer equilibrium. The oligomeric state of D-Acid/L-Base in 8 M urea was confirmed to be a monomer by sedimentation equilibrium analysis ($MW_{app} = 3300$; average expected $MW_{monomer} = 3698$). Urea denaturation of individual peptides showed that the homomeric structures formed by D-Acid and L-Base unfolded at low urea concentrations ($c_M \approx 1$ M urea; data not shown). Therefore, the homomeric structures should not contribute significantly to the monomer−tetramer equilibrium, as the tetramer would be the predominant species at low urea concentrations while the monomers would be the predominant species at higher urea concentrations.

A small but reproducible change in the CD ellipticity of the folded and unfolded states allowed for monitoring of the unfolding transition (Figure 3A). D-Acid/L-Base exhibited a cooperative unfolding transition, with a c_M of approximately 5.5 M urea (Figure 3A). The observed denaturation was fully reversible, as shown by diluting the peptide mixture in 9.5 M urea to lower urea concentrations (unpublished results). Fitting the denaturation profile to a monomer−tetramer equilibrium resulted in a $\Delta G°_{fold}$ of -29.3 ± 0.7 kcal/mol, corresponding to a total peptide concentration of ~100 nM for half the peptides to be unfolded. The same value of $\Delta G°_{fold}$ within experimental error was obtained with peptide concentrations of 40 and 80 μM (unpublished results).

Testing the Helical Net Packing Model. The importance of the relative half-heptad shift of D-Acid and L-Base (Figure 1C) was tested by comparing the stabilities of the D-Acid/L-Base complex and the D-Acid/unshift-L-Base complex, where unshift-L-Base is a peptide with an unshifted heptad register compared with D-Acid (i.e., both peptides start at heptad position **f**; Figure 1C). Helical net analysis predicts that the two helical ends of D-Acid and unshift-L-Base would be structurally misaligned by a half-heptad, thus forming a structure less stable than D-Acid/L-Base (Figure 1A).

The D-Acid/unshift-L-Base complex denatures at a c_M of approximately 4.5 M urea, which is ~1 M lower than that of D-Acid/L-Base (Figure 3A). (The unfolding of D-Acid/unshift-L-Base at low urea concentrations precluded a reliable

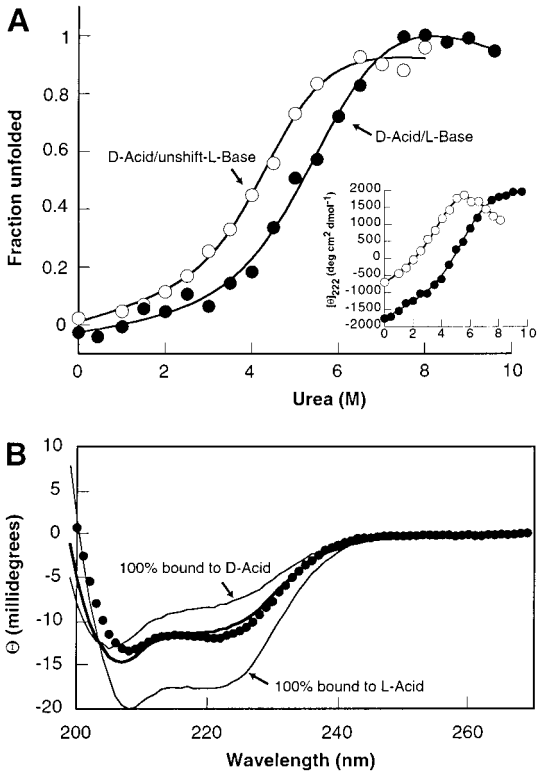

FIGURE 3: The D-Acid/L-Base tetramer is stable. (A) Urea denaturation of D-Acid/L-Base and D-Acid/unshift-L-Base, shown as fraction unfolded (main panel) and as molar CD ellipticity (inset). Conditions were 40 μM total peptide in PBS at pH 7.0. (B) Competition between D-Acid and L-Acid for L-Base (each peptide at 10 μM), as monitored by CD spectroscopy. The CD spectrum of a 1:1:1 mixture of D-Acid, L-Acid, and L-Base is shown (●). Also drawn are expected spectra for $f_D = 0$ (bottom line), $f_D = 1$ (top line), and $f_D = 0.66$ (thick line), where f_D is the fraction of L-Base bound to D-Acid. Calculations of the expected spectra are described in Materials and Methods.

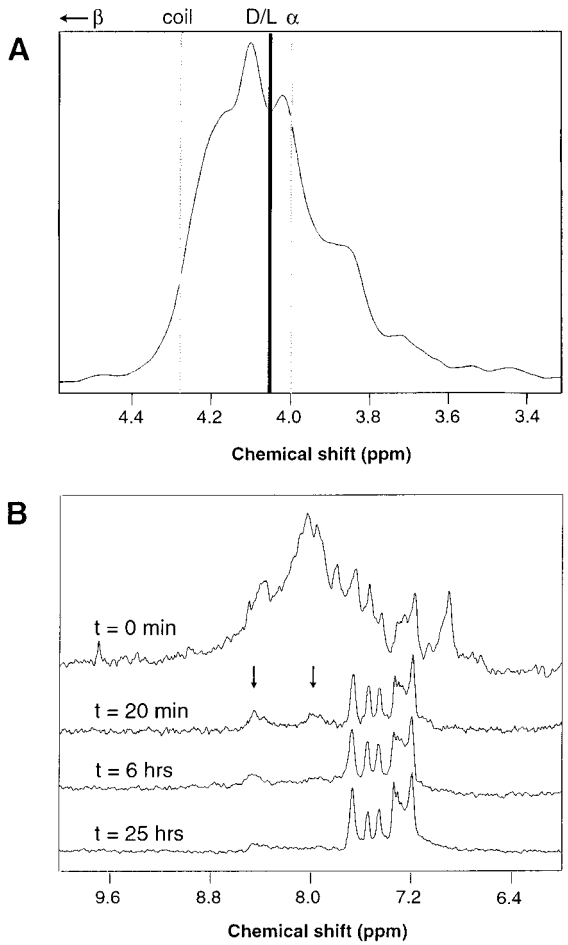

FIGURE 4: One-dimensional ^{1}H NMR studies of D-Acid/L-Base. (A) α-Proton region of D-Acid/L-Base. The observed average chemical shift (thick line) and the expected average chemical shifts for 100% helix, 100% random coil, and 100% β-strand are shown. (B) Hydrogen−deuterium amide-proton exchange of the D-Acid/L-Base tetramer. Shown are the spectra (starting from top) at 0 min, 20 min, 6 h, and 25 h (∞ time point). The arrows point to the most protected resonances.

estimate of the baseline of the folded structure and hence an accurate determination of $\Delta G°_{fold}$.) Moreover, sedimentation equilibrium analysis of D-Acid/unshift-L-Base shows incomplete formation of a tetramer (Figure 2C), as well as nonrandom residuals when fit to an idealized species model. The destabilization of the D-Acid/unshift-L-Base complex is consistent with the predictions of the helical packing model, providing strong evidence that the D-Acid/L-Base interface contains some specific knobs-into-holes packing.

Relative Stability of D-Acid/L-Base versus L-Acid/L-Base. The stability of the D-Acid/L-Base complex relative to that of the L-Acid/L-Base complex was directly assessed by a competition experiment (L-Acid in this report is termed Acid-pLL as in ref *21*, with all Leu residues at the **a** and **d** positions). Here, the efficacy of D-Acid in competing with L-Acid for their mutual partner (L-Base) was gauged by measuring a CD spectrum of a stoichiometric mixture of D-Acid, L-Acid, and L-Base at equilibrium. The result is compared with the expected CD spectra for cases of 100% L-Base bound to D-Acid and 100% L-Base bound to L-Acid (for example, the expected CD spectrum of 100% L-Base bound to D-Acid is the sum of the CD spectra of D-Acid/L-Base and free L-Acid). The CD spectrum of the mixture shows that D-Acid/L-Base and L-Acid/L-Base tetramers are comparable in stability, with ~66% of the L-Base preferentially bound to D-Acid (Figure 3B).

Secondary Structure of D-Acid/L-Base As Determined by NMR. The presence of both D- and L-amino acids in D-Acid/L-Base precludes the use of CD spectroscopy in estimating secondary structure content. For an estimate of overall secondary structure, a one-dimensional ^{1}H NMR spectrum of the D-Acid/L-Base complex was obtained. Previous studies established a strong relationship between the secondary structure of an amino acid and its α-proton chemical shift (*26*). Compared with random coil values, α-protons in α-helical conformations tend to be shifted upfield, while those in β-strand conformations tend to be shifted downfield. For D-Acid/L-Base, the expected average α-proton chemical shift is 4.27 ppm for 100% random coil, 4.76 ppm for 100% β-strand, and 4.00 ppm for 100% α-helix. The α-proton region of D-Acid/L-Base (Figure 4A) shows an overall upfield shift relative to the random coil values, with an average chemical shift of 4.05 ppm. No α-proton resonances are observed in the region expected for β-strand. This suggests D-Acid/L-Base is highly helical.

Hydrogen Exchange of D-Acid/L-Base. The dynamics of the hydrophobic core of the D-Acid/L-Base tetramer was investigated by hydrogen−deuterium amide-proton exchange. Although more than 90% of the protons exchange to

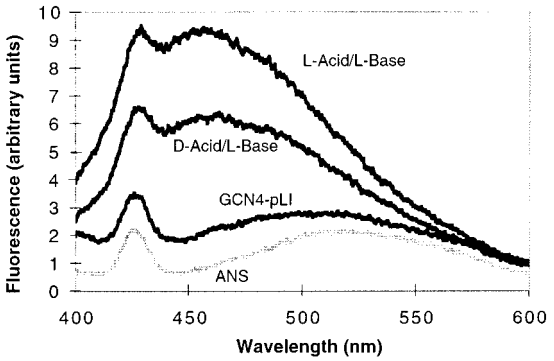

FIGURE 5: Solvent accessibility of the hydrophobic core of various tetramers as determined by binding to the nonpolar fluorophore ANS. From top to bottom are L-Acid/L-Base, D-Acid/L-Base, GCN4-pLI (*7*), and ANS alone. GCN4-pLI is a 33-residue peptide that forms a well-packed homotetramer (*7*). The total peptide concentration was 50 μM with 5 μM ANS. The peak at 429 nm is the Stokes shift of water from the Raman effect.

deuterium quickly, the slowest exchanging protons of the tetramer (indicated by arrows in Figure 4B) exhibit a half-life of approximately 3 h. This corresponds to a protection factor of 10^5 (see Materials and Methods), comparable to that of protected amide protons in well-packed proteins. Exchange due to a global unfolding mechanism, as determined by urea denaturation (Figure 2C), predicts a protection factor of 10^3 for the slowest exchanging protons (see Materials and Methods). The slowest exchanging amide protons of D-Acid/L-Base therefore have protection factors larger than that expected from global unfolding, a phenomenon often observed in naturally occurring globular proteins (*21*, *27*). [The 2 order of magnitude increase in stability of the most protected protons compared with that predicted from global unfolding may be due to residual structure in the unfolded state and an increase in protein stability in D_2O (*27*). Deviations from a strictly two-state transition may also underestimate ΔG°_{fold} at 0 M in the linear extrapolation method.] The observed protection factor for D-Acid/L-Base is 3 orders of magnitude larger than the protection factor of 10^2 reported for L-Acid/L-Base (*21*).

ANS Binding Studies. To characterize further the extent of solvent exposure in the entire hydrophobic core, the binding of the nonpolar fluorophore (ANS) to the tetramer was studied. Binding of ANS to hydrophobic patches on proteins induces a large increase in the magnitude of the fluorescence signal. The D-Acid/L-Base tetramer binds less ANS than the loosely packed L-Acid/L-Base tetramer, but more ANS than the well-packed GCN4-pLI tetramer (*7*) (Figure 5). Combined with the amide exchange results, this suggests that the D-Acid/L-Base heterotetramer contains a small, tightly packed hydrophobic core surrounded by more solvent-exposed hydrophobic residues. This is consistent with the helical packing model in Figure 1A, which predicts greater solvent accessibility for the **a** and **d** residues at the two end heptads than for residues in the two middle heptads.

Helix Orientation in D-Acid/L-Base. Coiled coils with L-amino acids are known to pack in both parallel and antiparallel orientations (*11*, *12*), typically with a preference for the parallel orientation. As with coiled coils, the antiparallel orientation in a D/L structure is also allowed by the helical net model ($\Omega = 180°$). The relative orientation of the two L-Base helices in the D-Acid/L-Base heterotetramer

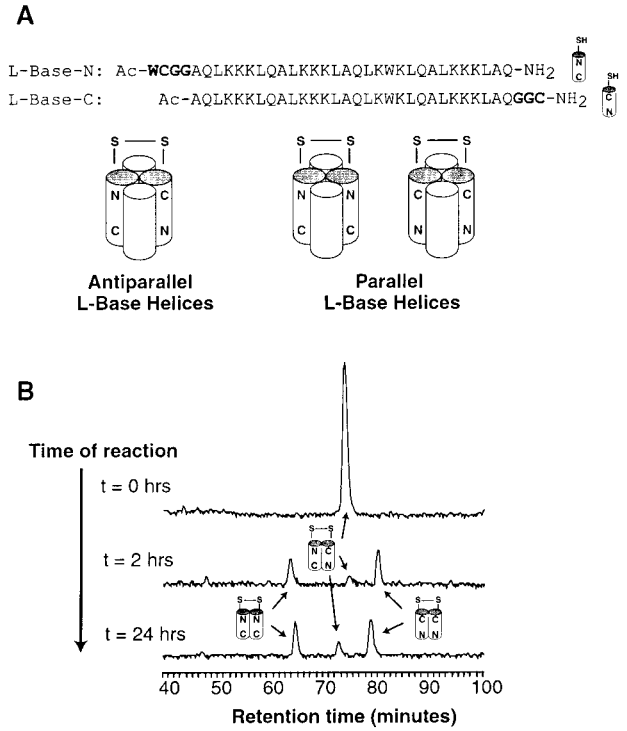

FIGURE 6: Determination of the relative orientation of the two L-Base helices in the D-Acid/L-Base heterotetramer. (A) The 5 μM L-Base-C (L-Base with a C-terminal Gly-Gly-Cys sequence) and 5 μM L-Base-N (L-Base with an N-terminal Trp-Cys-Gly-Gly sequence; the extra Trp facilitates its identification) are added to 10 μM D-Acid. The redox buffer (see Materials and Methods) allows the peptide monomers and disulfide bonds to rearrange. The presence of L-Base homodimers (L-Base-C or L-Base-N) would indicate a parallel helix orientation, while the presence of an L-Base heterodimer (L-Base-C/L-Base-N) would indicate an antiparallel helix orientation. In a tetramer of alternating D- and L-helices, an all-parallel or all-antiparallel packing arrangement between L-Base and D-Acid would result in the presence of only parallel L-Base dimers, while a mixture of parallel and antiparallel orientations for L-Base and D-Acid would result in the presence of both parallel and antiparallel L-Base dimers. (B) The analytical HPLC spectra of the starting antiparallel L-Base dimer (top); spectra for reactions after 2 h (middle) and 24 h (bottom) are also shown. The identities of all species were confirmed by LC−MS. Arrows point to the two parallel L-Base dimers, L-Base-N and L-Base-C. The presence of both parallel and antiparallel L-Base species indicates that in the D/L tetramer, D-Acid and L-Base pack in both parallel and antiparallel arrangements.

was determined by disulfide bond formation (*7*, *21*) (Figure 6A). Experiments were performed in a redox buffer that allowed peptide monomers and disulfide bonds to rearrange.

Analysis of the products by LC−MS shows the presence of both parallel and antiparallel arrangements for the L-Base helices in the tetramer, with the parallel orientation favored over the antiparallel orientation by a ratio of 5:1 (Figure 6B). The observed 5:1 preference was obtained starting with an oxidized antiparallel heterodimer (Figure 6), and also starting with the two individual oxidized parallel homodimers (unpublished results). A control reaction carried out in 4 M guanidine hydrochloride yielded the expected parallel to antiparallel preference of 1:1 (unpublished results). This parallel:antiparallel ratio is similar to that of the two L-Base helices in the L-Acid/L-Base system (*21*). The presence of the antiparallel arrangement of the two L-Base helices suggests that D-Acid packs against L-Base in the tetramer in both parallel and antiparallel orientations. Therefore, a left-

handed helix can pack against a right-handed helix in both the parallel and antiparallel orientations.

DISCUSSION

Structure of a D/L Tetramer. On the basis of the heteromeric Acid/Base system and the helical net model for helical packing, we designed and studied two peptides, D-Acid and L-Base, which form a stable, helical heterotetramer. This structure represents a novel protein motif which contains interacting left-handed and right-handed helices.

Biophysical data suggest that the D-Acid/L-Base tetramer contains both specific and nonspecific packing. Most of the hydrophobic core is loosely packed, as judged by its binding to the nonpolar fluorophore ANS, and the rapid exchange of the majority of amide protons. Moreover, the low chemical shift dispersion in the NMR spectrum of D-Acid/L-Base likely reflects the fluctuating character of a large portion of the protein complex in addition to the homogeneity in amino acid composition. Nevertheless, evidence also points to the presence of a small, well-packed hydrophobic core. First, a small number of amide protons are highly protected from exchange with solvent, exhibiting protection factors characteristic of well-packed proteins. Further, the increase in fluorescence upon addition of ANS is smaller for D-Acid/L-Base than for the loosely packed L-Acid/L-Base. Last, the destabilization of the structure upon shifting the sequence of L-Base by a half-heptad strongly suggests that some specific packing exists, in accord with the helical net model.

The presence of specific and nonspecific packing in the all-Leu core of the D-Acid/L-Base complex is consistent with published crystallographic data. For example, a racemic mixture of a designed α-helical peptide, designated Alpha-1, forms alternating sheets of left-handed and right-handed helices (*28*). In the hydrophobic leucine layer between the left-handed and right-handed helices of Alpha-1, half the Leu side chains are observed to pack in a knobs-into-holes fashion, while the other half fail to contact the opposing helix. For both the Alpha-1 and D-Acid/L-Base systems, a fully complementary interface would likely necessitate the abandonment of a simple and nonspecific all-Leu core.

Similarly, another study demonstrates that nonspecific hydrophobic forces are insufficient to drive the assembly of left-handed and right-handed helices. In this study, a two-helix peptide was designed, consisting of an N-terminal helix made of hydrophobic L-amino acids, followed by a linker, and a C-terminal helix made of hydrophobic D-amino acids (*29*). The crystal structure shows that although the two helices form the predicted right-handed and left-handed α-helices, they fail to associate with each other to form the intended hairpin structure (*29*). Further, intermolecular contacts appear to be dominated by hydrogen bonds rather than hydrophobic interactions. The inability of hydrophobic residues in preformed α-helices in this system to mediate intra- or intermolecular associations again suggests that some specific hydrophobic packing is necessary to drive the assembly of left-handed and right-handed helices.

Helical Net Model for Side Chain Packing. The mode of packing between left-handed and right-handed helices was investigated with two peptides, L-Base and unshift-L-Base, which differ in sequence by a relative half-heptad shift. In accord with the prediction of the helical net packing model, D-Acid/L-Base was more stable than D-Acid/unshift-L-Base, as judged by urea denaturation and sedimentation equilibrium analysis. The rough depiction of side chain packing in helical net diagrams is therefore applicable for D/L structures as well as for coiled coils with L-amino acids, although the detailed structural packing is surely different in D/L complexes.

It should be noted that the predictions of the helical net model for a dimer can be directly extended to trimers and tetramers. Like the GCN4-p1 dimer (*6*), crystal structures of GCN4-derived trimers and tetramers exhibit knobs-into-holes packing between the side chains of pairs of helices (*7*, *10*). Moreover, in all three oligomeric states, side chain packing occurs through the same interactions (Figure 1A). For example, a side chain at position **2a** of one helix interacts with side chains at positions **1d**, **1g**, **2a**, and **2d** in the neighboring helix. Therefore, the essential features of the helical net model, the interhelix packing angle and the manner of knobs-into-holes packing, are preserved in higher-order oligomers.

Knobs-into-holes packing for a D/L tetramer in three dimensions is demonstrated in a molecular model of the D/L tetramer (S. K. Sia, A. E. Keating, and P. S. Kim, unpublished results). To build such a model, the relative geometry of straight α-helices was systematically varied, and a conformational search was used to identify the best packing rotamers for an all-Leu core. The lowest-energy structure illustrates that a D/L heterotetramer with knobs-into-holes packing can be constructed for 30-residue peptides. Consistent with the biophysical data, the molecular model contains some native-like packing of side chains in the middle heptads, but loose packing of side chains in most instances.

Structural Specificity. A challenge frequently encountered in protein design is the engineering of conformational specificity in addition to thermodynamic stability. Specificity in coiled coils stems partly from the precise complementarity of buried hydrophobic residues (*7*, *10*), and to a larger extent from buried polar interactions and salt bridges that mildly destabilize the native structure but strongly destabilize alternate conformations (*30*). For example, an internal buried Asn interaction in the GCN4 Leu zipper is responsible for maintaining the register of the two helices (*6*, *7*). Also, the replacement of a core Leu with an Asn in L-Acid/L-Base switches a nonunique, loosely packed, but very stable tetramer to a specific, well-packed, and moderately stable dimer (*13*, *21*).

The introduction of a buried polar interaction in D-Acid-p1/L-Base-p1 expectedly destabilizes the complex. However, D-Acid-p1/L-Base-p1 does not form a well-packed, parallel heterodimer as in the case of the L version of Acid-p1/Base-p1. This difference in behavior likely reflects the difference in the specific packing of the hydrophobic core (including the core Asn residues) in D/L structures compared with coiled coils.

Moreover, in the L version of Acid/Base, the absence of buried polar interactions results not only in a loosely packed hydophobic core but also in the loss of structural uniqueness as shown by the lack of a unique orientation of the helices (*21*). The loss of a unique helix orientation is also observed for D-Acid/L-Base, as shown by the presence of both parallel and antiparallel arrangements for L-Base in the disulfide exchange experiment.

Clearly, a critical challenge in the design of D/L structures is to engineer conformational packing of the hydrophobic core. To force a specific orientation of helices, residues at the **e** and **g** positions can be chosen to form the most favorable salt bridge patterns in the desired orientation (*11*). One can also introduce different polar residues in the core (other than Asn in this study), which may favor a specific helix orientation (*12*) and also impart specific packing in the hydrophobic core (*30*). In addition, the packing of the hydrophobic core can be improved by using a variety of hydrophobic residues in addition to Leu. However, the specific packing of side chains for D/L structures is clearly different compared with that of coiled coils comprised of L-amino acids. Therefore, a selection of appropriate hydrophobic residues will likely require computational side chain repacking algorithms (*19*, *31*−*33*) instead of relying on the simple geometric rules observed for the packing of different hydrophobic residues in coiled coils (*7*, *10*).

Potential Applications. A potential use for the D/L structural motif is the design of protease-resistant D-peptides that bind natural protein targets. In this study, D-Acid effectively competes with L-Acid for their mutual target (L-Base) in a direct competition experiment. For real protein targets, the abandonment of a simple all-Leu interface on the D-peptide will be necessary to achieve stable and specific packing between the D-peptide and the target protein. The residues of the D-peptide at the binding interface can be selected by combinatorial methods such as mirror-image phage display (*34*, *35*) and synthetic peptide libraries (*36*). Alternatively, a possible computational approach involves first positioning the backbone of the helical D-peptide against the protein target in the manner described by the helical packing model (Figure 1A) to allow for favorable knobs-into-holes interactions among the side chains. This can be followed by a computational selection of the side chains on the helical D-peptide that pack most favorably against the protein target, using one of a number of side chain repacking algorithms (*19*, *31*−*33*).

The feasibility of finding biologically potent helical D-peptides is underscored by a number of known examples. The prevalence of helix/helix interactions at protein/protein interfaces (*37*) has allowed for the design of short, helical peptides and peptidometics as dissociative inhibitors against human immunodeficiency virus (HIV) protease, HIV reverse transcriptase, herpes simplex virus ribonucleotide reductase, and *Eco*RI (reviewed in ref *38*). Short, circular D-peptides that bind in a helical fashion to the helical region of the HIV-1 gp41 ectodomain have been identified using mirror-image phage display (*34*, *35*). Helical D-peptides that bind strongly to calmodulin have also been found (*39*). A detailed structural understanding of helical D/L heteromeric complexes will therefore aid in the future design of helical inhibitors containing D-amino acids against natural protein targets.

CONCLUSION

We designed and synthesized a protein complex consisting of left-handed and right-handed helices. The two peptides, D-Acid and L-Base, form a stable heterotetramer exhibiting features of both specific and nonspecific packing. A model describing the mode of packing between left-handed and right-handed helices is proposed, based on the knobs-into-holes packing model for coiled coils. This model may prove useful in designing helical D-peptide inhibitors and natural protein targets.

ACKNOWLEDGMENT

We gratefully acknowledge J. Pang and M. Burgess for peptide synthesis, Dr. P. Carr for help with NMR, L. Gaffney for editorial assistance with the manuscript, and Dr. A. Keating, Dr. M. Kay, and members of the Kim lab for helpful discussions and insightful comments on the manuscript.

REFERENCES

1. Kohn, W. D., Mant, C. T., and Hodges, R. S. (1997) *J. Biol. Chem. 272*, 2583−2586.
2. Lupas, A. (1996) *Trends Biochem. Sci. 21*, 375−382.
3. Crick, F. H. C. (1953) *Acta Crystallogr. 6*, 689−697.
4. Bowie, J. U. (1997) *Nat. Struct. Biol. 4*, 915−917.
5. Walther, D., Springer, C., and Cohen, F. E. (1998) *Proteins 33*, 457−459.
6. O'Shea, E. K., Klemm, J. D., Kim, P. S., and Alber, T. (1991) *Science 254*, 539−544.
7. Harbury, P. B., Zhang, T., Kim, P. S., and Alber, T. (1993) *Science 262*, 1401−1407.
8. Lau, S. Y. M., Taneja, A. K., and Hodges, R. S. (1984) *J. Biol. Chem. 259*, 539−544.
9. Gonzalez, L., Woolfson, D. N., and Alber, T. (1996) *Nat. Struct. Biol. 3*, 1011−1018.
10. Harbury, P. B., and Kim, P. S. (1994) *Nature 371*, 80−83.
11. Monera, O. D., Zhou, N. E., Lavigne, P., Kay, C. M., and Hodges, R. S. (1996) *J. Biol. Chem. 271*, 3995−4001.
12. Oakley, M. G., and Kim, P. S. (1998) *Biochemistry 37*, 12603−12610.
13. O'Shea, E. K., Lumb, K. J., and Kim, P. S. (1993) *Curr. Biol. 3*, 658−667.
14. Graddis, T. J., Myszka, D. G., and Chaiken, I. M. (1993) *Biochemistry 32*, 12644−12671.
15. Betz, S. F., Bryson, J. W., and DeGrado, W. F. (1995) *Curr. Opin. Struct. Biol. 5*, 457−463.
16. Schafmeister, C. E., LaPorte, S. L., Miercke, L. J. W., and Stroud, R. M. (1997) *Nat. Struct. Biol. 4*, 1039−1046.
17. Handel, T. M., Williams, S. A., and DeGrado, W. F. (1993) *Science 261*, 879−885.
18. Gonzalez, L., Plecs, J. J., and Alber, T. (1996) *Nat. Struct. Biol. 3*, 510−515.
19. Harbury, P. B., Plecs, J. J., Tidor, B., Alber, T., and Kim, P. S. (1998) *Science 282*, 1462−1467.
20. DeGrado, W. F., Summa, C. M., Pavone, V., Nastri, F., and Lombardi, A. (1999) *Annu. Rev. Biochem. 68*, 779−819.
21. Lumb, K. J., and Kim, P. S. (1995) *Biochemistry 34*, 8642−8648.
22. Edelhoch, H. (1967) *Biochemistry 6*, 1948−1954.
23. Laue, T. M., Shah, B. D., Ridgeway, T. M., and Pelletier, S. L. (1992) in *Analytical Ultracentrifugation in Biochemistry and Polymer Science* (Harding, S. E., Rowe, A. J., and Horton, J. C., Eds.) pp 90−125, The Royal Society of Chemistry, Cambridge, U.K.
24. Johnson, M. L., Correia, J. J., Yphantis, D. A., and Halvorson, H. R. (1981) *Biophys. J. 36*, 575−588.
25. Bai, Y., Milne, J. S., Mayne, L., and Englander, S. W. (1993) *Proteins 17*, 75−86.
26. Wishart, D. S., Sykes, B. D., and Richards, F. M. (1991) *J. Mol. Biol. 222*, 311−333.
27. Bai, Y., Milne, J. S., Mayne, L., and Englander, S. W. (1994) *Proteins 20*, 4−14.
28. Patterson, W. R., Anderson, D. H., DeGrado, W. F., Cascio, D., and Eisenberg, D. (1999) *Protein Sci. 8*, 1410−1422.
29. Karle, I. L., Banerjee, A., and Balaram, P. (1997) *Folding Des. 2*, 203−210.
30. Hendsch, Z. S., Jonsson, T., Sauer, R. T., and Tidor, B. (1996) *Biochemistry 35*, 7621−7625.

31. Dahiyat, B. I., and Mayo, S. M. (1996) *Protein Sci. 5*, 895−903.
32. Ghirlanda, G., Lear, J. D., Lombardi, A., and DeGrado, W. F. (1998) *J. Mol. Biol. 281*, 379−391.
33. Koehl, P., and Delarue, M. (1994) *J. Mol. Biol. 239*, 249−275.
34. Schumacher, T. N., Mayr, L. M., Minor, D. L., Milhollen, M. A., Burgess, M. W., and Kim, P. S. (1996) *Science 271*, 1854−1857.
35. Eckert, D. M., Malashkevich, V. N., Hong, L. H., Carr, P. A., and Kim, P. S. (1999) *Cell 99*, 103−115.
36. Lam, K. S., Lebl, M., and Krchnak, V. (1997) *Chem. Rev. 97*, 411−448.
37. Stites, W. E. (1997) *Chem. Rev. 97*, 1233−1250.
38. Zutshi, R., Brickner, M., and Chmielewski, J. (1998) *Curr. Opin. Chem. Biol. 2*, 62−66.
39. Fisher, P. J., Prendergast, F. G., Ehrhardt, M. R., Urbauer, J. L., Wand, A. J., Sedarous, S. S., McCormick, D. J., and Buckley, P. J. (1994) *Nature 368*, 651−653.

BI010725V